Pattern formation and selection in quasi-static fracture

Kwan-tai Leung*[1] and Zoltan Néda†[2]
[1] *Institute of Physics, Academia Sinica, Taipei, Taiwan 11529, R.O.C.*
[2] *Department of Theoretical Physics, Babeş-Bolyai University, str. Kogalniceanu nr. 1, RO-3400 Cluj-Napoca, Romania*

(Last revised February 1, 2008)

Fracture in quasi-statically driven systems is studied by means of a discrete spring-block model. Developed from close comparison with desiccation experiments, it describes crack formation induced by friction on a substrate. The model produces cellular, hierarchical patterns of cracks, characterized by a mean fragment size linear in the layer thickness, in agreement with experiments. The selection of a stationary fragment size is explained by exploiting the correlations prior to cracking. A scaling behavior associated with the thickness and substrate coupling, derived and confirmed by simulations, suggests why patterns have similar morphology despite their disparity in scales.

PACS numbers: 05.65.+b, 62.60.Mk, 46.50.+a

Nature is full of fascinating patterns [1]. A ubiquitous yet relatively less explored class of patterns is that produced by the fracture of solids [2], as often seen in cracked structures, battered roads and dried out fields. Although there have been early observations and characterizations [1,3,4], only rather recently has it been studied systematically [5–9]. The mathematical problem of a network of interacting cracks [11] is a formidable one, in view of the difficulties facing a lone crack propagating in a homogeneous medium [10]. One way to make progress is to turn to a statistical description. This view has been pursued extensively in investigations of the fracture of disordered media [12], borrowing concepts such as percolation and universality from studies of phase transitions. For crack patterns, an immediate observation is the geometrical similarities of patterns over a wide range of scales, from microns [5] to kilometers [3]. This suggests some universal mechanism is at work and microscopic details may be unimportant. Hence, analogous to phase transitions, a mesoscopic, coarse-grained description may be sufficient and more useful than a microscopic one, provided essential features are captured.

Crack patterns often arise from slow physical (e.g., embrittlement, contraction) or chemical (e.g., oxidation) variations, or their combination, in the material properties of an overlayer on top of an inert substrate. The overlayer may fail in different ways [14], such as decohesion, buckling, spalling and in-plane cracking. In this paper, we address the pattern-selection aspects of quasi-static, in-plane cracking by identifying the dominant mechanism and control parameters that determine the ensuing patterns. By understanding a simplified, coarse-grained model, we hope to achieve the same for the phenomena in general.

A Bundle-Block Model – In a mesoscopic approach, the grains in the overlayer are represented by an array of blocks. Each pair of *neighboring* blocks is connected by a bundle of H bonds (coil springs) each of which has spring constant $k \equiv 1$ and relaxed length l. Initially, the blocks are randomly displaced by $\vec{r} = (x, y)$, where $|\vec{r}| \ll l$, about their mean positions on a triangular lattice. For slow cracking on a frictional substrate, the motion of the grains is overdamped, the system evolves quasi-statically with driving rate much slower than relaxation rate. In this case, we need not solve the equations of motion but instead may update the configurations according to threshold criteria specified below.

In typical crack formations, the layer often hardens and/or weakens in time; it tends to contract but is resisted by friction from the substrate. As a result, stress is built up and relaxed slowly. The simplest way to incorporate these effects is first to pre-strain the array by $s = (a - l)/a > 0$, where $a \equiv 1$ and $l < a$ are the initial and final grain spacing, respectively. Then, two thresholds, F_s for slipping and F_c for cracking, are decreased systematically to induce slipping and cracking. This rule is more general than it seems: As the evolution of the model is determined entirely by the ratios between forces and thresholds, hardening, weakening *and* their combination amount to this same rule. Since the thresholds decrease by the same physical means, their ratio $\kappa \equiv F_c/F_s$ remains fixed. In a drying experiment, the narrowing and breaking of liquid bridges between grains, due to evaporation, may provide a physical picture of this driving. Even though there may not be an exact correspondence in experiments, and other drivings are conceivable [13], our choice is physically relevant and sufficiently simple to allow for some analytic understanding.

The general expression of the force is rather complicated, it results in slow updating. Since in realistic situation the stress is primarily tensile and the strain $s \ll 1$, to a good approximation we expand the force to first order in $\vec{r}$ to obtain a Hookean form for the force components on a block:

$$F_x = \sum_{i=1}^{6} H_i[asC_i + (x_i - x)(sS_i^2 + C_i^2) +$$

$$(y_i - y)(1-s)S_iC_i], \quad (1)$$

where the index i labels the six nearest neighbors and the associated bundles, and the constants $C_i = \cos[(2i-1)\pi/6]$ and $S_i = \sin[(2i-1)\pi/6]$. F_y may be obtained from F_x by interchanges $x \leftrightarrow y$, and $C_i \leftrightarrow S_i$.

Initially, the system is globally stable. In discrete simulation steps t, it evolves according to these rules:

1. The thresholds are lowered until either is exceeded somewhere in the system;
2. if $F \equiv \sqrt{F_x^2 + F_y^2} > F_s$, the block slips to a mechanically equilibrium position where $F \equiv 0$;
3. if the bond tension $> F_c$ in a bundle of H_i bonds, $H_i \to H_i - 1$ provided the bundle has not been damaged in the same step.

The system relaxes until global stability is restored. This constitutes one *simulation step or one event*. In rule 3, we break no more than one bond/bundle/step in order to avoid instantaneous downward propagation of cracks before the neighboring stress field has ever relaxed. Otherwise, spurious long and vertical microcracks would be generated which do not conform to real systems. The progressive damage of the bundle mimics successive breakage of liquid bridges, hence H plays the role of the local thickness [15]. Our algorithm is designed to take advantage of the dominance of the horizontal propagation of cracks, due to the presence of the top, free surface.

Results and Discussions – Throughout this work, square systems are used with linear size $20 \le L \le 300$, $s \le 0.1$, and free boundary conditions (FBC) are imposed [16]. In the $\kappa - H$ subspace, the time evolution can be divided into three qualitatively distinct phases:

I. The system contracts by slippings, the slip size (total number of slippings in an event) grows in time;

II. There are slippings and bond breakings, the system is progressively damaged, then fragmented, while contraction continues;

III. Bond-breaking saturates, fragmentation stops, slipping dominates as block spacing converges to the equilibrium value l.

A typical evolution is shown in Fig. 1. The main feature of phase I is the growth of correlations. Since everything depends on F_s, we need to know how it varies first. Its decay rate is governed by the density of F near F_s among the L^2 blocks, where $0 \le F < F_s$. To a first (mean-field) approximation, this density is F_s/L^2. Hence $F_s(t) - F_s(t+1) \propto F_s(t)/L^2$, leading to $F_s(t) \propto e^{-t/\tau}$ with a decay constant $\tau \sim L^z$ and a mean-field prediction $z_{\rm MF} = 2$. Numerically, we find $z = 1.80 \pm 0.03$, reflecting the finite, albeit weak, spatial correlation among the seeds that initiate distinct events.

Now we derive the growth laws for the strain field and the slip size. Due to the diminishing threshold, slippings start from the free edge and invade into the bulk, giving rise to a strain-relieved peripheral region of width denoted by ξ. The strain increases from the boundary toward the bulk, reaching the bulk value s (see Fig. 2(a)). To determine its profile, consider for the moment a one-dimensional version: the force on the $i^{\rm th}$ block is given by $F_i = (a - l + x_{i+1} - x_i)H - (a - l + x_i - x_{i-1})H = (s_i - s_{i-1})H$. Hence $F = Hds/du$, where u is the distance from the edge. Metastability of the system requires $Hds/du < F_s$ but of the same order. Thus we obtain for general dimensions the growth of the invasion length

$$\xi(t) \approx \frac{\xi_0 sH}{2F_s(t)}, \quad (2)$$

with constant $\xi_0 = O(1)$. For a finite system of size L, the invasion saturates (i.e., $\xi = L$) when $F_s \le F_s^{\rm sat} = \xi_0 sH/L$, or equivalently $t \ge t_{\rm sat} = \tau \ln(H/F_s^{\rm sat})$. As a result, the global maximum strain $s_{\rm max}$ in the system drops continuously thereafter (see Fig. 2(b)):

$$s_{\rm max} = \begin{cases} s & t < t_{\rm sat} \\ \frac{LF_s}{\xi_0 H} & t > t_{\rm sat}. \end{cases} \quad (3)$$

As $\xi(t)$ grows, so does the mean slip size, $S(t)$, as required by energy balance. The total energy relieved over the strain-relieved region is of the order $U = \xi L s^2 H/2$. It is dissipated by friction during slippings. Since the slip distance is $\alpha F_s/H$ [8] where $\alpha = 1/3(1+s)$ [17], each block slip dissipates an energy $\alpha F_s^2/2H$. The total dissipation is then $E = \int_0^t dt' S(t') \alpha F_s(t')^2/2H$. Equating E to U and differentiating with respect to t, we readily find

$$S(t) = S_0 \left(\frac{H}{F_s(t)}\right)^3 \qquad t < t_{\rm sat}, \quad (4)$$

where the prefactor $S_0 = \xi_0 s^3 L/2\alpha\tau$. Since the invasion is independent of L, we have $\xi_0 \sim L^0$ and hence $S_0 \sim L^{1-z}$. For $t > t_{\rm sat}$, $S(t)$ saturates to a constant $S_{\rm sat} = S_0(L/s\xi_0)^3 \sim L^\eta$ which diverges as $L \to \infty$: the system becomes critical with a nontrivial exponent $\eta > 0$. Put together, we obtain a "scaling relation"

$$\eta = 4 - z, \quad (5)$$

relating the dynamical and stationary behavior. From $z_{\rm MF} = 2$, we get $\eta_{\rm MF} = 2$. Simulations give $\eta = 2.20 \pm 0.03$ instead, in agreement with the independent estimate of z. From Eq. (4), it is evident that dynamic scaling $S(t; H, L) = L^\eta \Phi(H/LF_s(t))$ is obeyed, with the scaling function $\Phi(x \ll 1) \sim x^3$ and $\Phi(x \gg 1) =$const, as exhibited in Fig. 3.

Several remarks are in order: (i) $\eta > 2$ implies that each site slips an average $L^{\eta-2}$ times per event. Such repeated topplings are manifestations of system-wide correlations in the force variable. (ii) The connection between dynamics (z) and criticality (η) is attributed to energy

balance. Thus we believe similar relations also exist for other forms of driving. (iii) For finite κ, fracture eventually sets in before criticality is fully developed. However, even then, each fragment settles into a stationary, critical state characterized by the same η and its fragment size.

Moving on to phase II, an important question in fracture is how its onset is affected by material properties and external conditions. Apparently, fracture occurs when κF_s decreases below the bond tension s in the bulk, i.e.,

$$F_s \to F_s^* \approx \frac{s}{\kappa} \tag{6}$$

from above. Note that this result is independent of H, but the corresponding simulation step is: $t^* \approx \tau \ln(\kappa H/s)$, because $F_s \approx He^{-t/\tau}$. Hence, the substrate and the thickness have the same effect on the onset. The extra waiting time for thicker layers or more frictional substrates allows more slippings and hence stronger correlations at t^* – larger fragments are anticipated.

The difference in correlations is also reflected in the morphology of cracks. For very small κH, the substrate is very frictional or the layer very thin. Pinning is so strong that most avalanches are of size one. In a virtually uncorrelated stress environment, cracks soon appear but do not propagate. Fragmentation is resulted from percolation of microcracks. For $\kappa H \ll 1$, most bonds are ultimately broken to turn the system into powder.

Going up in κH, the larger friction or thickness allows stronger correlations up to fracture, measured by $\xi(t^*)$ and $S(t^*)$. Relaxation of stress field around crack tips becomes more effective, leading to more pronounced stress concentration and straight crack propagation. The resulting fragmentation process is hierarchical: after a cellular network is formed with the primary straight cracks, secondary cracks break the fragments into smaller ones, and so on. Cracks of later generations are more "diffusive" in character, they tend to wiggle and branch under smaller stresses [18], as there are more and more free boundaries. These features are exemplified in Fig. 4. At long times, fragmentation is complete, resulting in fragments with areas that fit a log-normal distribution (cf. [8]), and a mean area $A \sim H^2$ (see below). Experimentally, morphology may be characterized by the distribution $P(\theta)$ of crack angle θ at a joint. A shift of the peak position from $\theta \approx 90^\circ$ to 60° as thickness decreases has been observed in amorphous media [6]. Although the usefulness of $P(\theta)$ is limited by lattice anisotropies in our model, a direct comparison with real patterns (see Fig. 4) produced by slow drying of cornstarch-water mixtures (to be reported elsewhere) reveals striking similarities. Furthermore, the linear dependence of A on thickness agrees with previous experiments [6,7].

As κH is increased further, the question of fracture or not arises. Fracture is possible only if $\kappa F_s(t) < s_{\max}(t)$ at some t. From Fig. 2(b), this translates to the condition $\kappa F_s(t_{\rm sat}) \equiv s$ (equivalently $t_{\rm sat} \equiv t^*$). A critical system size $L_c(\kappa, H) = \xi_0 \kappa H$ emerges, below which a system never cracks at fixed κ and H. Equivalently, a finite system of size L does not crack if $\kappa H > L/\xi_0$. This again agrees with the basic experimental fact that a sufficiently small and thick layer does not crack. Now, given that a system of size $L > L_c$ cracks, the next, even more interesting question of pattern selection is when fragmentation stops. We do not have a rigorous answer, as the dynamics of interacting cracks is complicated, but we argue that it stops when the system has broken up into fragments of typical size $O(L_c)$. This gives $A(\kappa, H) \sim (\kappa H)^2$. This argument implies the memory of the correlations at the onset persists in the *final* fragmented state, reminiscent of the generation of quenched disorder in systems with metastability and frustration [19] – both features crucial to surface fracture. Excellent scaling behavior in simulations (Fig. 5) strongly supports this scenario.

In summary, we study a bundle-block model for quasistatic, in-plane fracture. Guided by experiments, we incorporate two factors that dictate the pattern-forming process – the substrate and thickness – by means of two control parameters. The ensuing pattern, however, is characterized mostly by one scaling variable. Self organization of the strain field prior to fracture is derived and shown to dictate the properties of the pattern, particularly to select the fragment size. Our results answer, at least qualitatively, why thin layers crack finely and thick ones do not crack at all, and why similarities are accompanied by a variability of scales. Supported by experimental observations, our model appears to capture the salient features of real systems, so that despite the use of a specific form of driving, the ideas may apply to other situations generally dominated by stick-slip motion.

We thank Yves Bréchet and Eric To for useful discussions, and C.K. Chan for help on experiment. This work is partially supported by the National Science Council of R.O.C.

---

* E-mail: leungkt@phys.sinica.edu.tw
† E-mail: zneda@hera.ubbcluj.ro

[1] P.S. Stevens, "Patterns in nature", Atlantic Monthly Press (1974).
[2] B. Lawn, "Fracture of brittle solids", 2nd ed., Cambridge Univ. Press (1993).
[3] J.T. Neal, A.M. Langer and P.F. Kerr, Geol. Soc. Am. Bull., **79**, 69 (1968).
[4] J. Walker, Sci. Am. **255**, 178 (1986).
[5] A. T. Skjeltorp and P. Meakin, Nature **335**, 424 (1988); J. V. Andersen, Y. Bréchet and H. J. Jensen, Europhys. Lett. **26**, 13 (1994); T. Hornig, I.M. Sokolov and A. Blumen, Phys. Rev. E **54**, 4293 (1996); K.M. Crosby and R.M. Bradley, *ibid.* **55**, 6084 (1997); J.V. Andersen, D. Sornette and K.-t. Leung, Phys. Rev. Lett. **78**, 2140 (1997).
[6] A. Groisman and E. Kaplan, Europhys. Lett. **25**, 415

(1994).
[7] Y. Bréchet, D. Bellet and Z. Néda, Key Eng. Mat. **103**, 247 (1995).
[8] K.-t. Leung and J. V. Andersen, Europhys. Lett. **38**, 589 (1997).
[9] S. Kitsunezaki, Phys. Rev. E **60**, 6449 (1999).
[10] J.S. Langer and A.E. Lobkovsky, J. Mech. Phys. Solids **46**, 1521 (1998); and refs. therein.
[11] M. Kachanov, Adv. Appl. Mech. **30**, 259-438 (1994).
[12] H.J. Herrmann and S. Roux, eds., "Statistical models for the fracture of disordered media", North-Holland (1990).
[13] If the thresholds vary independently, fine tuning becomes necessary to produce nontrivial steady-state patterns [8]; no such tuning is evident in nature.
[14] J.W. Hutchinson, Adv. in Appl. Mech. **29**, 63 (1992).
[15] This is a trick to introduce the *effect* of thickness without incurring a demanding three-dimensional simulation.
[16] Partially and fully periodic boundary conditions are also considered. They lead to similar patterns with the same fragment-area statistics.
[17] α specifies the fraction of the force components distributed to neighbors in a slip. Note that without external driving, all force components are strictly conserved locally during slipping *and* cracking, for all s.
[18] Smaller initial strain leads to more diffusive cracks. Generally, typical straight-crack length increases with s.
[19] S. Boettcher and M. Paczuski, Phys. Rev. Lett. **79**, 889 (1997); and refs. therein.

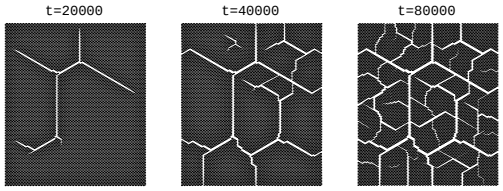

FIG. 1. Snapshots for $L = 100$, $s = 0.1$, $\kappa = 0.5$, $H = 9$. Note the progression from straight to diffusive cracks.

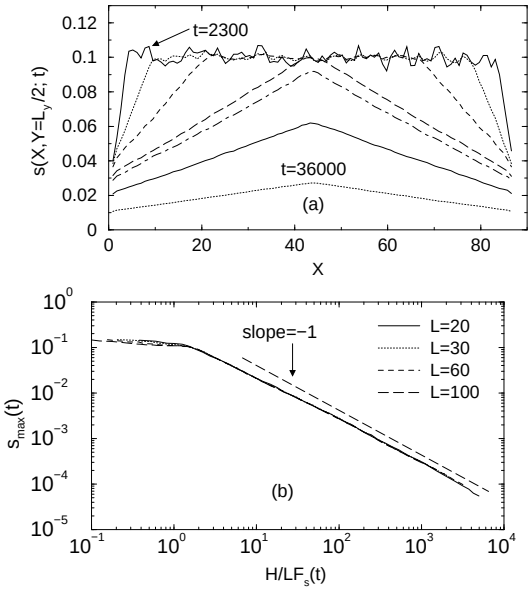

FIG. 2. (a) Strain field profiles show progressive strain relief as t increases for $L = 100$, $s = 0.1$, $H = 2$, $\kappa = \infty$. It leads to temporal variation of the maximum strain in (b).

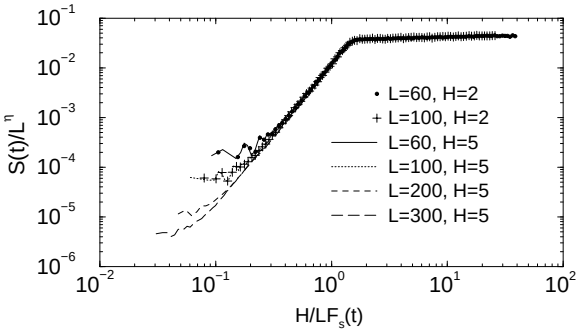

FIG. 3. Dynamic finite-size scaling of mean slip size toward criticality. $s = 0.1$, $\kappa = \infty$, $\eta = 2.2 \pm 0.03$.

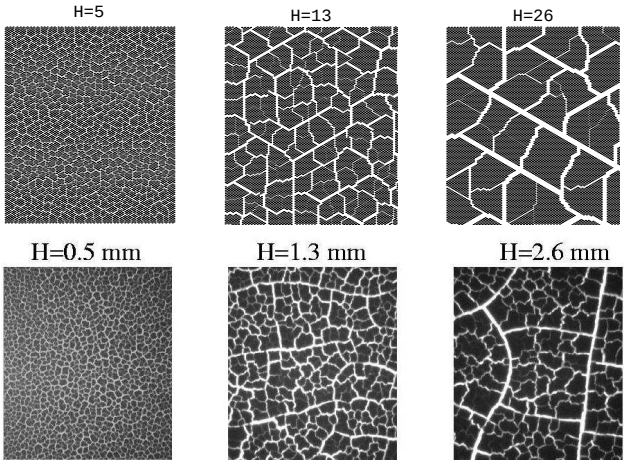

FIG. 4. Stationary patterns at different thickness. Upper row: by simulation, $L = 100$, $s = 0.1$, $\kappa = 0.25$. Increasing κ at fixed H has the same effect. Lower row: from slow-drying experiment of cornstarch-water mixture with thickness matching that of simulation.

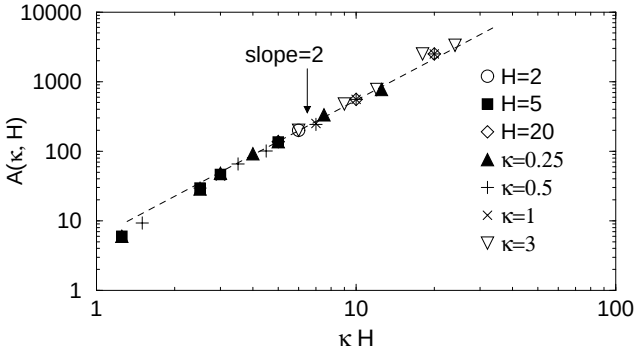

FIG. 5. Substrate-thickness scaling of mean fragment area. $L = 100$, $s = 0.1$, with either fixed κ or H.